

Supporting Information

Fluid-powered rotation-contact separation hybrid triboelectric nanogenerator for heavy metal ion removal and corrosion protection

Xinyi Ji ^a, Yukun Liu ^a, Lina Zhou ^a, Zekang Zhang ^a, Chao Yang ^b, Zhenyuan

Xu ^a, Dongzhi Zhang ^{a,*}

^a State Key Laboratory of Chemical Safety, College of Control Science and Engineering, China University of Petroleum (East China), Qingdao 266580, China

^b Technology Inspection Center of Shengli Oilfield, China Petroleum & Chemical Corporation, Dongying 257000, China

*Corresponding author: Dongzhi Zhang

E-mail address: dzzhang@upc.edu.cn

Tel: +86-532-86982928

Fax: +86-532-86981335

Figure captions

Fig. S1. (a) RCS-TENG front view. (b) RCS-TENG rear view. (c) RCS-TENG top view.

Fig. S2. Contact Angle diagram of Ecoflex/ZnS material.

Fig. S3. (a) SEM image of the Ecoflex/ZnS composite. (b) The Zn element in Ecoflex/ZnS composite. (c) The S element in Ecoflex/ZnS composite.

Fig. S4. Graph of the relationship between the output and flow velocity of RCS-TENG and the error range of the average values of multiple measurements.

Fig. S5. (a) Long term stability of PG-TENG output voltage. (b) Long term stability of output current of PG-TENG.

Fig. S6. Comparison of direct charging and charging of 1 mF capacitors via EMM circuitry.

Fig. S7. (a) The relationship between the removal rate and time of Pb at different concentrations. (b) Physical image of Cd deposited on cathode titanium plate at different times.

Fig. S8. (a) The relationship between the removal rate of Cu and time at different spacings between the anode and cathode of the electrode plate; (b) The relationship between the removal rate of Pb and time at different spacings between the anode and cathode of the electrode plate; (c) The relationship between the removal rate of Cd and time at different spacings between the anode and cathode of the electrode plate.

Fig. S9. (a) EDS characterization of Cu adherents on titanium plate electrodes. (b) EDS characterization of Pb adherents on titanium plate electrodes. (c) EDS

characterization of Cd adherents on titanium plate electrodes.

Supporting Movie

Movie 1. LEDs with "TENG" mark are lit by RCS-TENG.

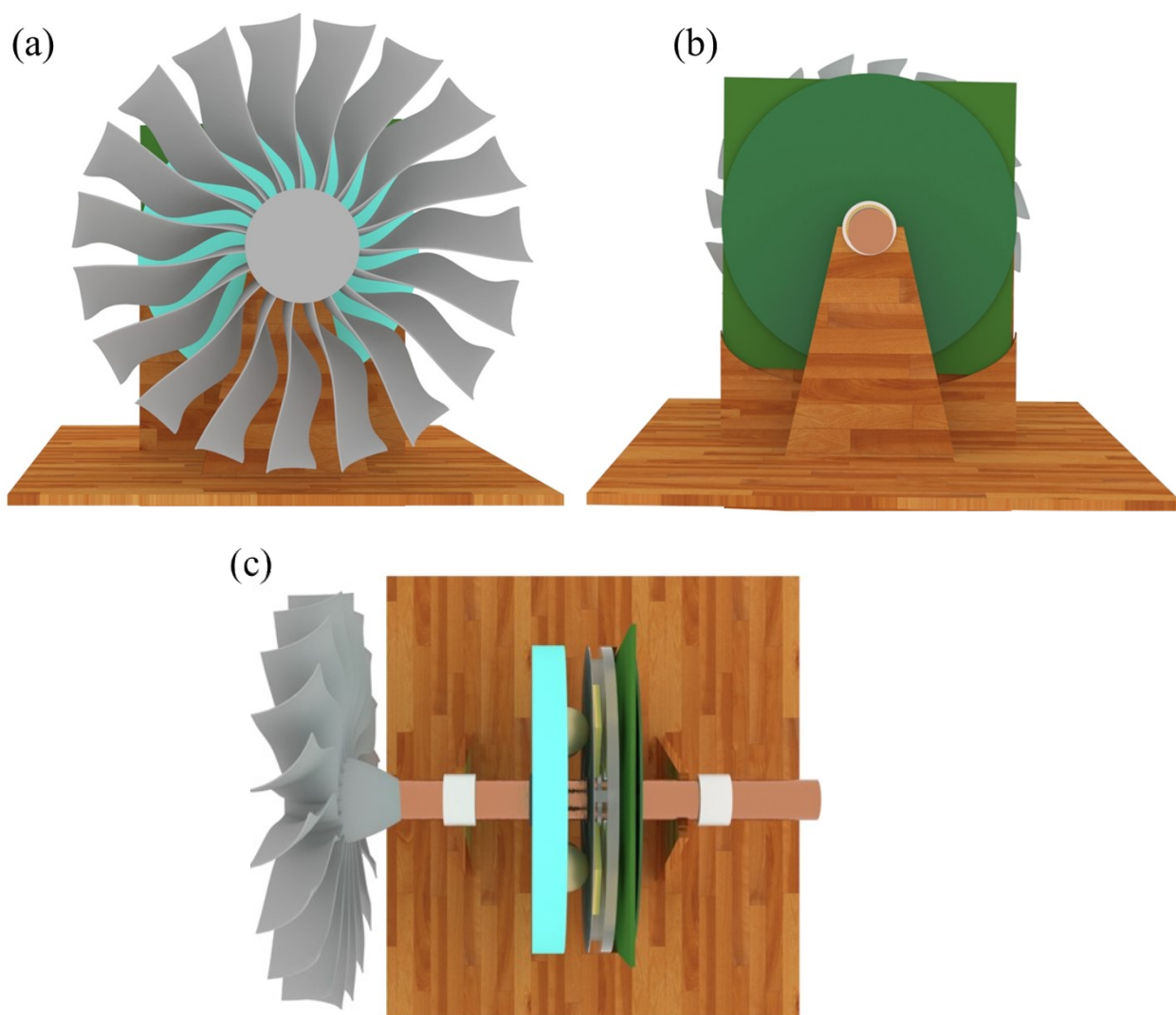


Fig. S1. (a) RCS-TENG front view. (b) RCS-TENG rear view. (c) RCS-TENG top view.

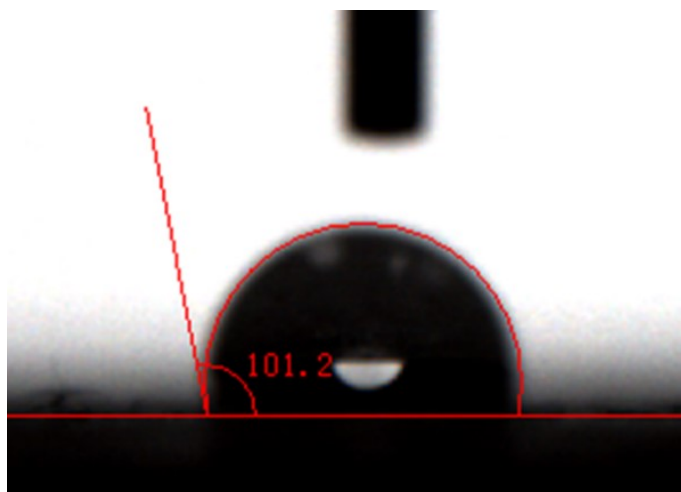


Fig. S2. Contact Angle diagram of Ecoflex/ZnS material.

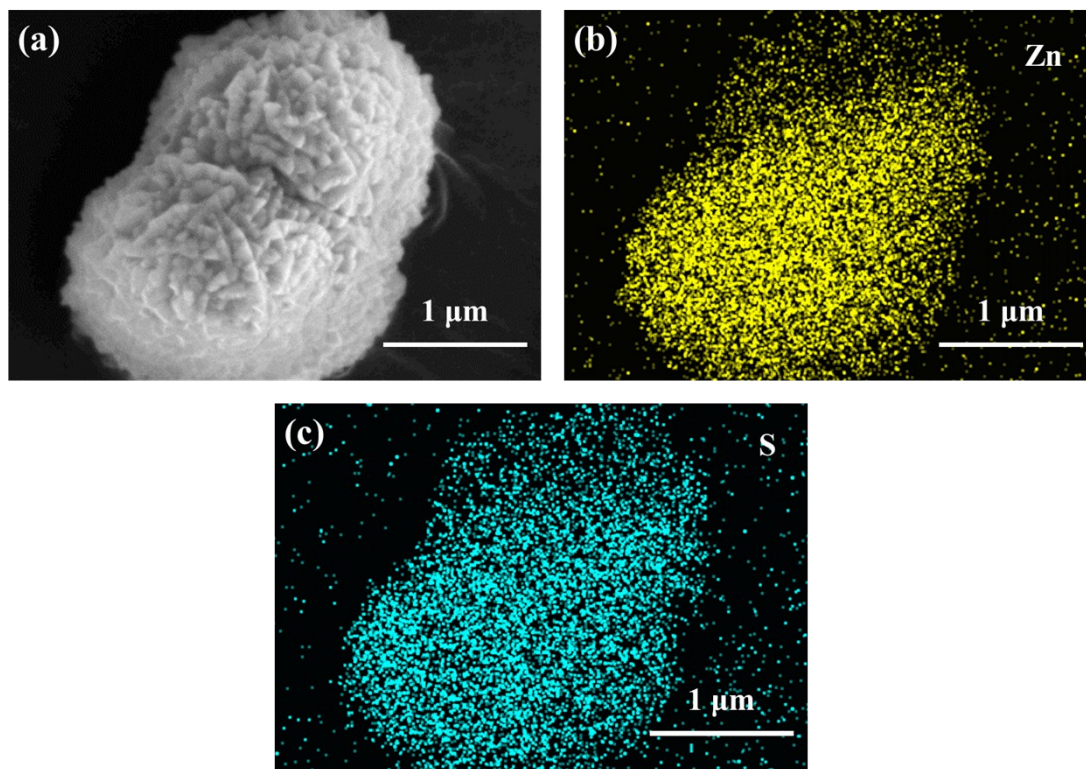


Fig. S3. (a) SEM image of the Ecoflex/ZnS composite. (b) The Zn element in Ecoflex/ZnS composite. (c) The S element in Ecoflex/ZnS composite.

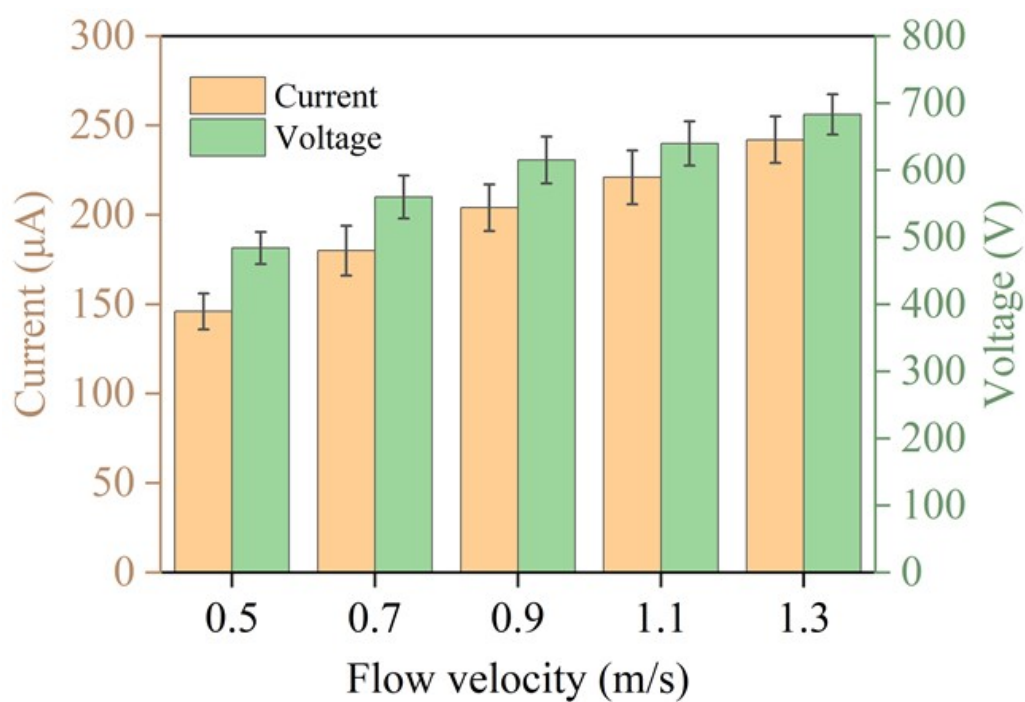


Fig. S4. Graph of the relationship between the output and flow velocity of RCS-TENG and the error range of the average values of multiple measurements.

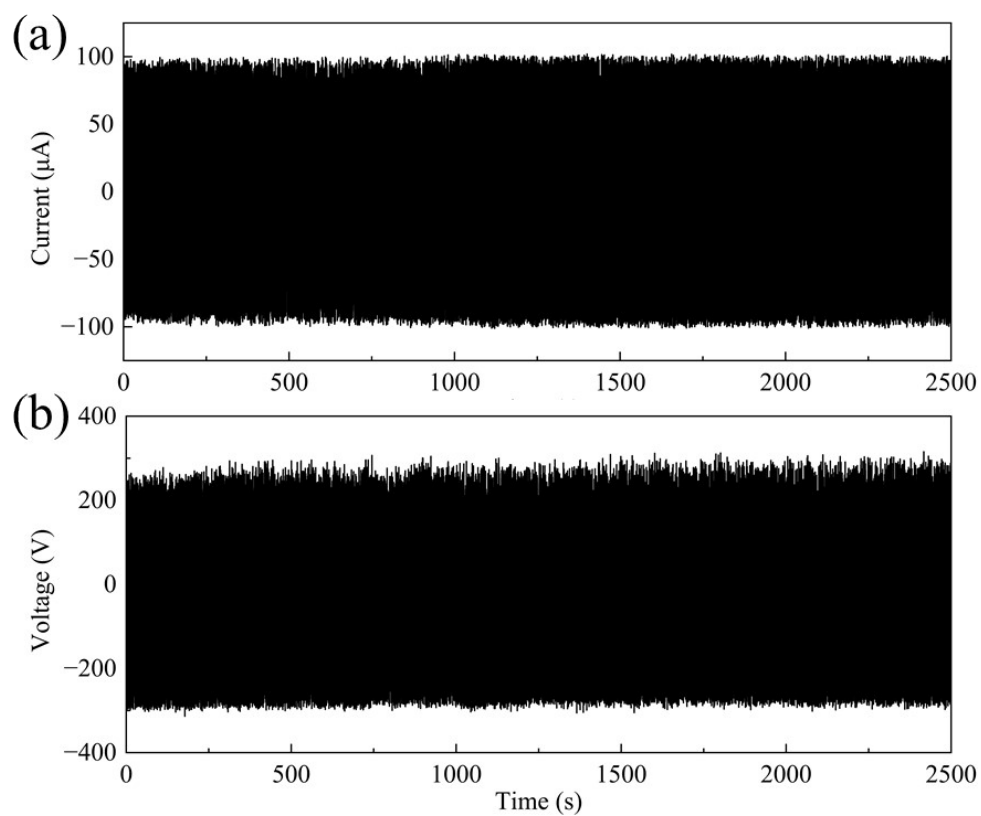


Fig. S5. (a) Long term stability of PG-TENG output voltage. (b) Long term stability of output current of PG-TENG.

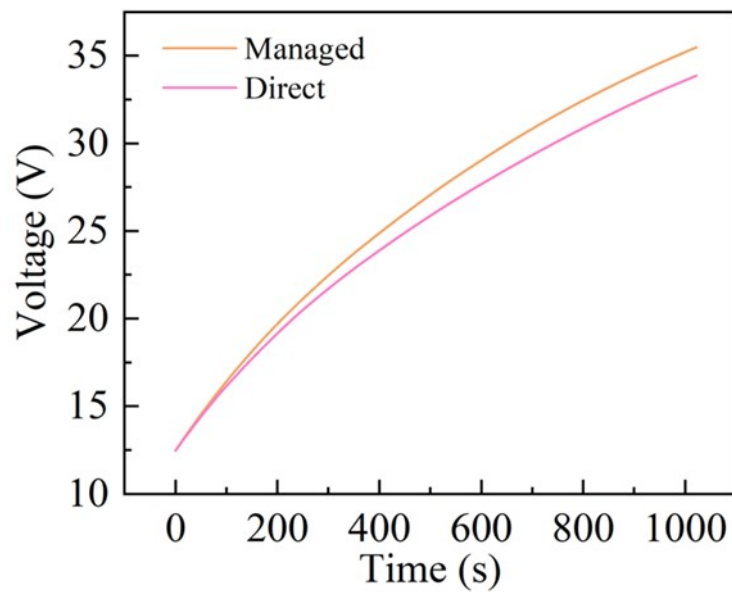


Fig. S6. Comparison of direct charging and charging of 1 mF capacitors via EMM circuitry.

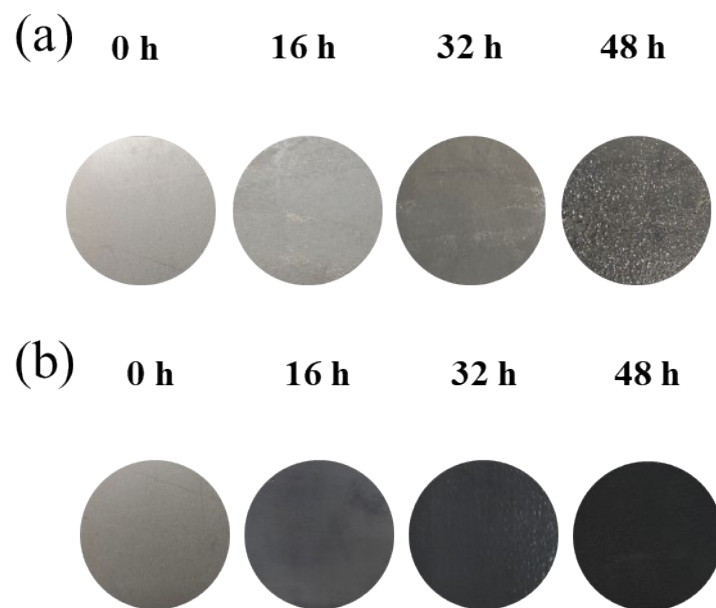


Fig. S7. (a) The relationship between the removal rate and time of Pb at different concentrations. (b) Physical image of Cd deposited on cathode titanium plate at different times.

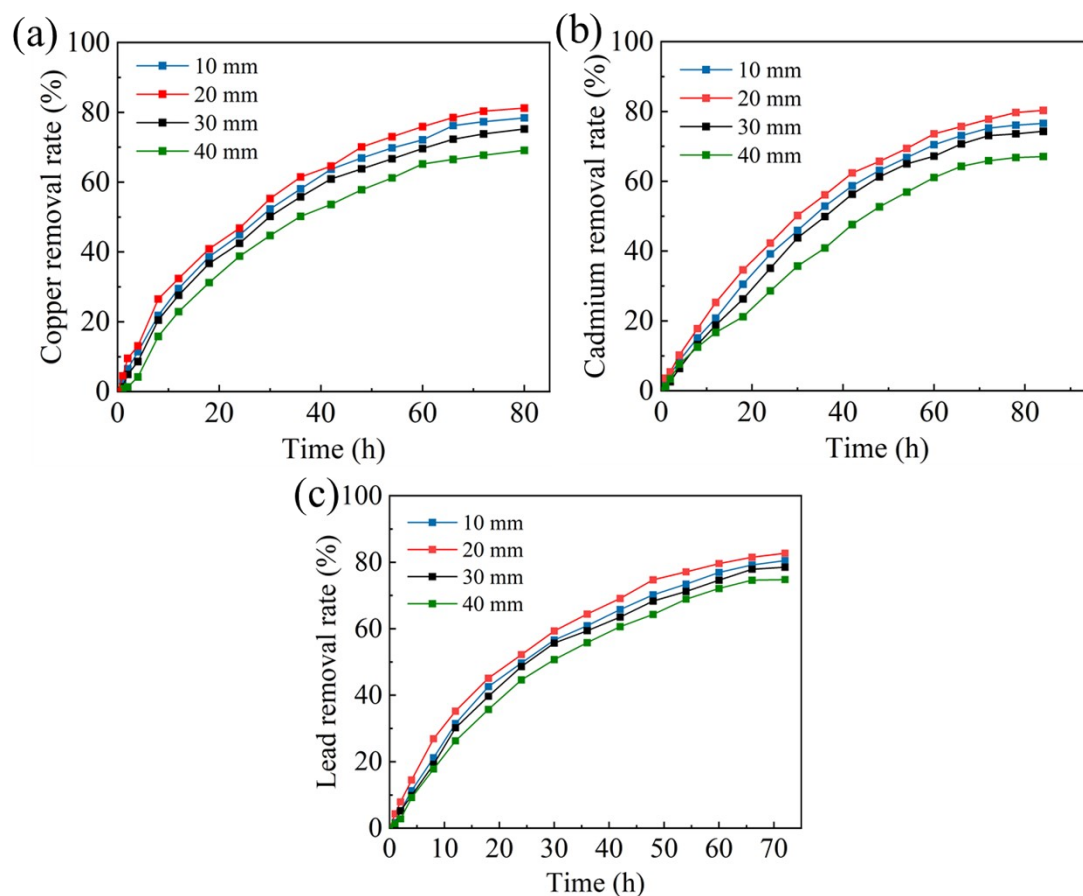


Fig. S8. (a) The relationship between the removal rate of Cu and time at different spacings between the anode and cathode of the electrode plate; (b) The relationship between the removal rate of Pb and time at different spacings between the anode and cathode of the electrode plate; (c) The relationship between the removal rate of Cd and time at different spacings between the anode and cathode of the electrode plate.

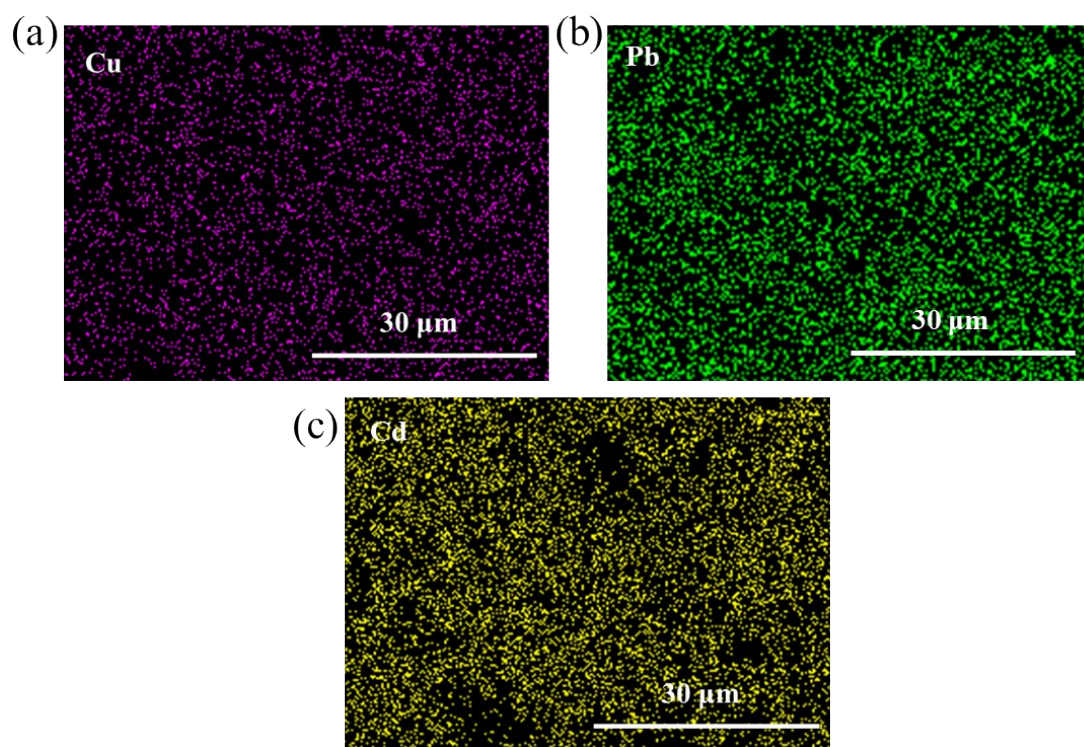


Fig. S9. (a) EDS characterization of Cu adherents on titanium plate electrodes. (b) EDS characterization of Pb adherents on titanium plate electrodes. (c) EDS characterization of Cd adherents on titanium plate electrodes.